Coastal change detection along the Fire Island, US under the impact of Hurricane Sandy based on LiDAR data

Zhou Yining[12], Tian Sijing[3,*], Wang Haoxue[4], Chang Chan[12], Gao Yanfang[12], Zhang Bimin[12], Wang Xueqiu[12]

[1]Key Laboratory of Geochemical Exploration, Institute of Geophysical and Geochemical Exploration, Ministry of Natural Resources, P. R. China
[2]UNESCO International Center on Global-scale Geochemistry
[3]College of Astronautics, Nanjing University of Aeronautics and Astronautics, Nanjing 211106, China
[4]Geo-Compass Information Technology Co., Ltd, Beijing 100089, China

KEY WORDS: Coastal erosion, LiDAR, Machine Learning, Digital Terrain Model (DTM), Coastline extraction, Disaster detection.

ABSTRACT:

Coastal erosion occurring all over the world is a disastrous coastal geological phenomenon. It can be caused by many natural factors such as wind and waves. Hurricane Sandy made landfall on the east coast of the United States at the end of October 2012 and caused severe damage to the economy and ecological environment. In this paper, we employ the ground-based LiDAR which has higher spatial resolution to observe the coastal change detection at Fire Island, New York where the place is severely affected. The research showed that sediment accumulation occurred away from the coast, up to 2.9 meters, erosion close to the coast, up to 9 meters. The total volume of the study area decreased by 78160.96 cubic meters. The coastline retreated by 32.86 meters on average. In addition, a website has been designed to record coastal erosion anytime and anywhere. We hope this study will help people better understand the impact of hurricanes on coastal erosion, enhance our awareness of environmental protection, and provide scientific information for further study.

1. INTRODUCTION

Coastal erosion occurs almost all over the world's coastlines and is defined as the gradual wearing away of the earth's surface by the action of natural forces of wind and water (Li et al., n.d.). Increasing storminess, continuous sea level rising and storm waves make it a serious problem along many countries (Swift, 1968; Swift and Thorne, 1991; Leatherman et al., 2000; Lentz et al., 2013; Prasad and Kumar, 2014; Obu et al., 2017; Gracia et al., 2018; Mohd et al., 2018; Li et al., n.d.). The coastal erosion problem has been attracting more attention from society because erosion along the coast may cause loss of coastal land and even dramatic landscape modification, etc.(Dolan et al., 1978; Marfai, 2011; Prasad and Kumar, 2014). In particular, hurricanes and tidal effects can cause coastal movement and erosion, the drastic changes of coastline cannot be ignored for the impact on ecology, environment, economy and society, so the study of coastline change and coastal erosion has received widespread attention.

Most studies in change detection such as coastal erosion studies commonly used satellite imageries or aerial photographs to observe and monitor, because Remote Sensing (RS) and Geographic Information System (GIS) offer convenient ways to model and visualize. Many researchers use high resolution images for coastline change detection and extraction, etc. Maglione suggested using WorldView-2 imagery with two indices of Normalized Difference Vegetation Index (NDVI) and Normalized Difference Water Index (NDWI) to extract coastline (Maglione et al., 2014). Li's team combined the spatial modeling and monitoring shoreline erosion with high-resolution imagery together along the south shore of Lake Erie. Light Detection and Ranging (LiDAR), a kind of remote-sensing technology, has been increasingly used and becomes an important tool in coastal geomorphology. In contrast to optical remote sensing, LiDAR can facilitate the acquisition of detailed, accurate topographic data over broad coastal regions. In addition, it works day and night without the influence of different light conditions, which makes it more convenient in change detection (Gálai and Benedek, 2017; Sofonia et al., 2019; Cui, 2020; Gibson et al., 2020; Xian et al., 2020; Zhu et al., 2020; Krishnan et al., n.d.). On the Atlantic coast, France government created a new observatory called OR2C of coastal hazards to monitor nearly 400km of coastal line based on airborne LiDAR technology. The data which is updated every year and freely accessible to coastal managers supported decision-making and updated policies or strategic documents (Kerguillec et al., 2019). Obu (2017) studied elevation and volume change used repeat airborne LiDAR with 1 m horizontal resolution to study elevation and volume change, coastline movements in the Yukon Coastal Plain (Canada). The ground object classification result of LiDAR data is improved by combining multi-features of imagery, thus, the verification LiDAR has outstanding ability in land and water differentiation. The impacts of hurricane Sandy on the shoreline and inner shelf, which are permanently submerged and primarily accessible only through acoustic mapping, are harder to observe. In this study, GIS, RS and machine learning are combined to get LiDAR data processed and visualized.

The objectives in this study are summarized as follows:

A. Derive DTMs for pre-storm and post-storm using XYZ ground-based LiDAR; Calculate (ECM) Elevation Change Model;
B. Extract coastlines for pre-storm and post-storm;

* Corresponding author

C. Develop a website for recording coastal erosion.

This paper is structured as followed. Study area is introduced in section 2. Data information is stated in section 3. Section 4 proposes DTMs process, the structure of the model and coastline extraction through Machine learning feature classification. Results and discussion are shown in section 5. Conclusions are presented in section 6.

2. STUDY AREA

Fire Island is a tiny island on the southern edge of New York's Long Island as Figure 1, which was severely destroyed by the high tides and winds caused by Hurricane Sandy. Sandy made landfall in New Jersey on October 30, 2012, causing great economic and social damage to the east coast of the United States. Sandy attained sustained wind speeds of 25.1 m/s and significant wave heights of 9.65 m. These values were ~25% and ~50% higher, respectively, than most other strong storms during this period (Sebek et al., 2014; Goff et al., 2015). It was the second-costliest hurricane in U.S. history, as it caused an estimated 75 billion dollars in economic damage (Varlas et al., 2019). Sandy caused high tides and high winds that seriously eroded the coasts of many coastal cities in the United States, the peak storm surge was at 3.9 m and the peak storm tide was at 4.4 m (Hsu, 2013).

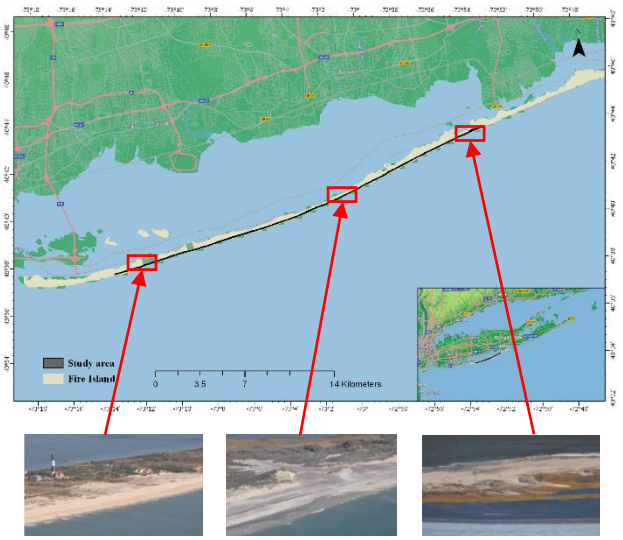

Figure 1. Study area Fire Island(Note: Map derived from ArcGIS Pro) and its three locations(Petersburg, 2015)

3. DATA

U.S. Geological Survey (USGS) aimed to characterize beach topography following substantial erosion that occurred during Hurricane Sandy. USACE-FRF team collected the high-resolution LiDAR data using the CLARIS platform. CLARIS is a vehicle-mounted system that integrates a terrestrial LiDAR scanner and X-band radar with precise motion and position information. In this study, we used point cloud data which was used to create the DTMs. The point cloud data was derived as ASCII format, which needed to convert to las format for the subsequent data processing. Table 1 lists the experimental data obtained. In addition, Google high-resolution images are also used to conduct the incipient object classification for training sample which applied to coastline extraction.

Data name	Data format	Acquisition time
Fire Island Point cloud data	ASCII XYZ Data	Oct 2012; Nov 2012
Fire Island boundary	Shapefile	May 2012

Table 1. Data information.

4. METHODS

4.1 DTM generation

To generate DTM of pre-storm and post-storm, LAStools are employed for XYZ data processing and Raster Calculate in ArcMap which is set for ECM calculation, data processing and visualization. The ECM was created as Figure 2.

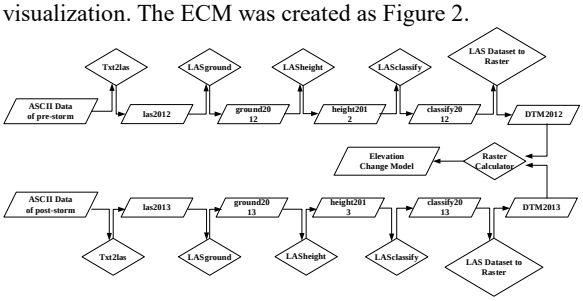

Figure 2. Elevation change model acquisition flow

Because of the large volume of TLS data, the effective use of this data inevitably involves some semi-automatic or automated methods. One of the available solutions is LAStools, which includes tools to classify, tile, convert, filter, raster, triangulate, contour and clip LiDAR data (Lederer et al., 2004; Jovan D. and Nikola Č., 2018; Moudrý et al., 2020).

Basic information of "las2012" could be acquired from LASinfo. The Z coordinate value varied from -0.57 to 15.39 and it only has one return. What's more, the point density is 3.81 per square meter while point spacing is 0.51 meters. Therefore, the file was set as multi-purpose datasets referenced to Figure 3 (Silke, 2012) .

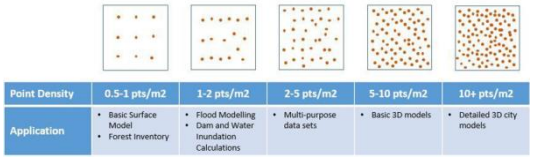

Figure 3. Common Point Densities (Felix, 2017)

4.1.1 Elevation Change Model: To derive Elevation change model, subtract the 2013 DTM from the 2012 DTM using Raster calculator. Therefore, we can determine the place where erosion occurs or sediment accumulation happens. The following Figure 4 is a schematic diagram of the ECM acquisition method. There are three types of value in ECM, the positive value in blue cells presents erosion while the negative value in green cells stands for deposition. Obviously, the orange cells represent there is no elevation change in that area.

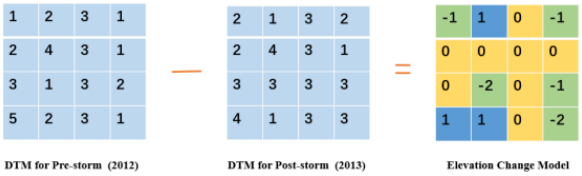

Figure 4. Schematic diagram of deriving Elevation change model

4.2 Coastline extraction

In this section, PCA (Principal Component Analysis) and SVM (Support Vector Machine) are applied to extract features and classify. PCA aims to transform multiple indexes into a few comprehensive indexes by using the idea of dimensionality reduction (Bishop, 1999; Shi and Zakhor, 2011; Lee et al., 2016; Pan et al., 2019). SVM is a kind of generalized linear classifier that classifies binary data by supervised learning(V. N. Vapnik, 1999; V. Vapnik, 1999; Lodha et al., 2006; Li et al., 2007; Samadzadegan et al., 2010; Matkan et al., 2014). For coastline extraction of LiDAR data, the LiDAR data in the study area are divided into four types according to the ground object classification system referencing to Google high-resolution images. The following Figure 5 is the flow chart of coastline extraction for LiDAR feature classification.

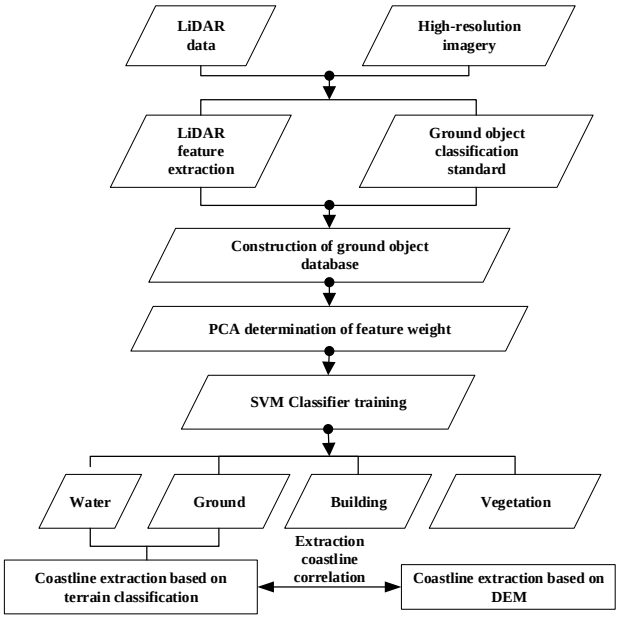

Figure 5. Coastline extraction flow chart

There are four types of targets respectively for water, ground, building and vegetation. The experiment uses the combination of feature echo intensity (EI), echo times (ET), point density (PD) and intensity density (ID). PCA weight determination for extracted combination features (CF) was set as the input of the classifier, to train the samples of LiDAR data and obtain the SVM classifier to achieve classification. To avoid accidental contingency, the experimental training and testing data are in different areas, and the database is shown in Table 2.

Class	Train	Test
Water	1300	325
Ground	1268	317
Building	1224	306
Vegetation	1120	280
Total Number	4912	1228

Table 2. Training test database

5. RESULTS AND DISCUSSION

5.1 Results

5.1.1 Coastal erosion change: Following the ECM, we could identify the area along the coast eroded, elevation lowered and deposition occurred far from the shoreline, elevation rose. It exists an obvious hierarchy from south to north no matter in which area as Figure 8-10. (Note: The maps are derived from ArcGIS Pro from partial Fire Island). Along the study area, which is about 3.1 km, the peak value was up to 13.6 and the lowest value was -0.8 m after the storm, while the peak value of elevation was 14.3 and the lowest value was -0.6 m before the storm. The average elevation was dropped by 0.66 m. 82% of the area experienced elevation dropped and collapsed.

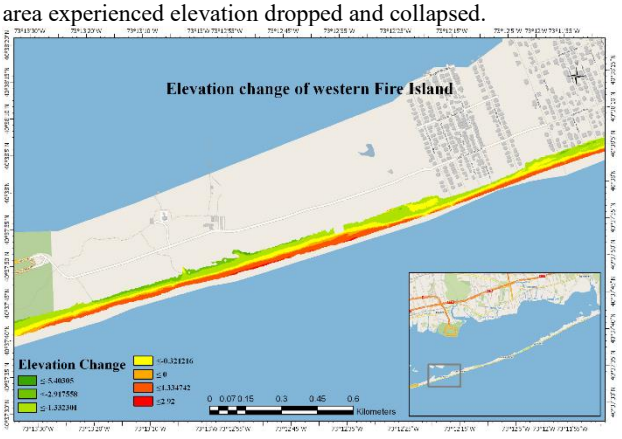

Figure 6. Elevation changes of western Fire Island

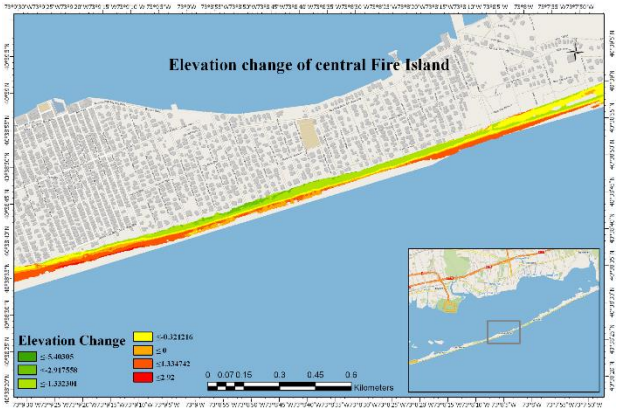

Figure 7. Elevation changes of central Fire Island

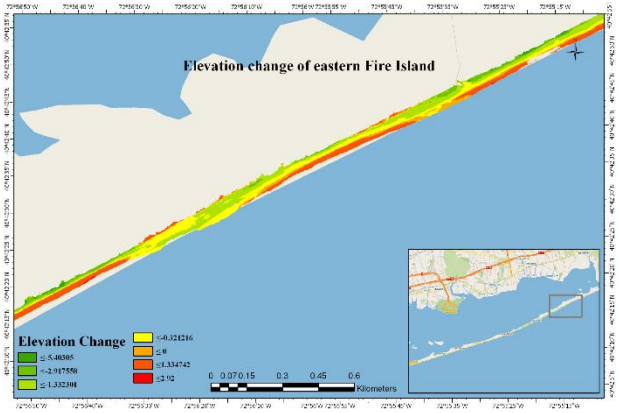

Figure 8. Elevation changes of eastern Fire Island

The total volume of the study area decreased by 78160.96 cubic meters while the surface area increased by 311343.18 square meters; the mean attitude of the study area decreased by about 0.82 meters.

5.1.2 Coastline movement: For this part, the average retreat of coastline is 32.86 m with a maximum of 63.28 m which happened in the eastern Fire Island, and the minimum value is 19.46 m which occurred in the western Fire Island.
As the basic data of GIS, the coastline extracted from DTMs is remarkably similar to that extracted from LiDAR data, thus confirming the reliability of coastline extraction by machine learning.

5.1.3 Website development: To raise users' awareness and better statistics on how often and where coastal erosion occurs, we develop a website (Story map) which employs HTML, CSS, PHP, PhpMyAdmin database and JavaScript for recording and updating coastal erosion around the world anytime. (Note: the link is https://arcg.is/19zGfL. The layers are encrypted at present, it can be emailed if you are interested in frames)

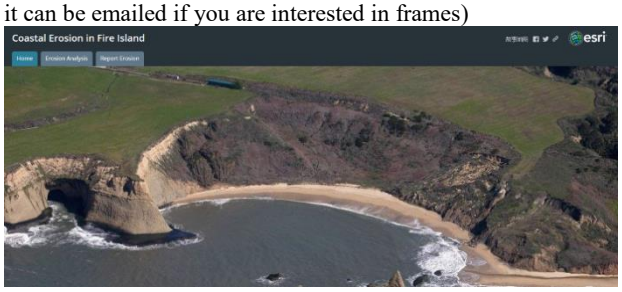

Figure 9. Website initial page (Note: Screen shot from website)

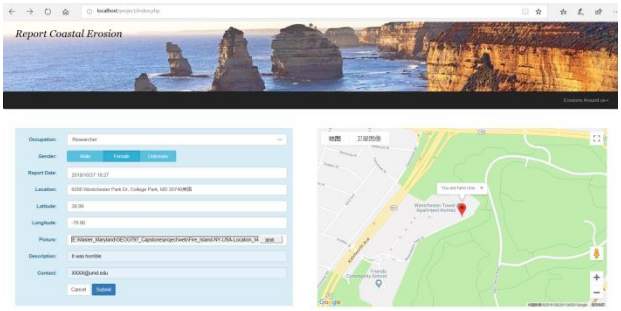

Figure 10. Website report page (Note: Screenshot from website)

5.2 Discussion

In this project, we figure out the place where are tends to occur sediment accumulation while areas elevation decrease. In addition, the coastline movement is observed using Machine learning feature classification. Therefore, after Hurricane Sandy leaves, more sediment accumulates in the littoral area, which contribute to more surface area of the beach.

5.2.1 Parameters in Point cloud data processing: There are many parameters in LAStools model making a difference to the outcome. Here, the parameter "No bulge" in LASground model is discussed as followed. We notice this parameter can contribute a lot when classifying the Lidar points into Unassigned or Ground points. When the parameter "No bulge" is applied in LASground tool, nearly 10 times as point clouds are classified into Unassigned as Figure 11. Therefore, the parameter "No bulge" is significant when using the terrestrial data because this tool is designed for airborne-LiDAR.

	Checking "No bulge" in lasground	Leaving "No bulge" as blank
Pre-storm las file cloud points classification	Classification Codes Classification / Point Count / % 1 Unassigned / 387,143 / 5.11 2 Ground / 7,185,585 / 94.89	Classification Codes Classification / Point Count / % 1 Unassigned / 38,791 / 0.51 2 Ground / 7,533,937 / 99.49
Post-storm las file cloud points classification	Classification Codes Classification / Point Count / % 1 Unassigned / 505,188 / 5.78 2 Ground / 8,227,376 / 94.21 5 High Vegetation / 420 / 0.00	Classification Codes Classification / Point Count / % 1 Unassigned / 75,196 / 0.86 2 Ground / 8,657,767 / 99.14 5 High Vegetation / 21 / 0.00
Pre-storm volume	Area_2D / Area_3D / Volume 1926000 / 1942369.960163 / 5745919.782763	Area_2D / Area_3D / Volume 1921924 / 1938158.122327 / 5776156.573625
Post-storm volume	Area_2D / Area_3D / Volume 2233598 / 2253713.042438 / 5667758.799217	Area_2D / Area_3D / Volume 2226676 / 2246157.364714 / 5802346.769899

Figure 11. Different results in LASground tool by applying "no bulge"

5.2.2 Parameters in the machine learning: The test results are shown in Figure 12, and the classification results are shown in Table 3.

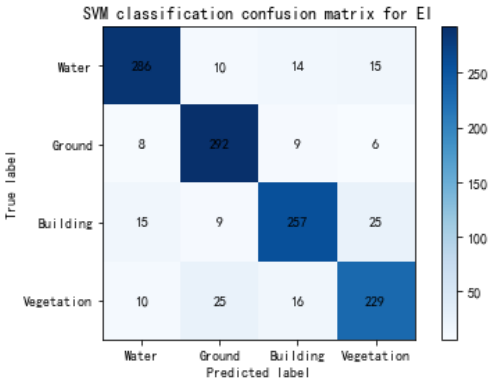

(a)

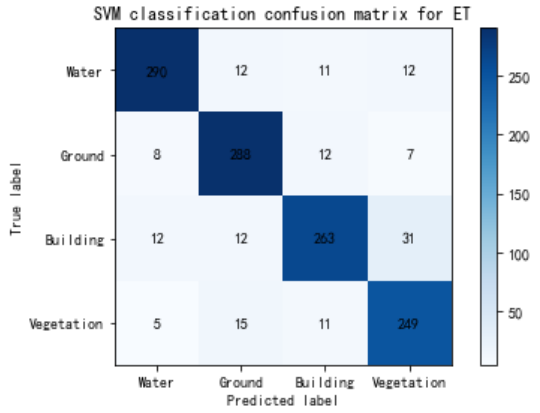

(b)

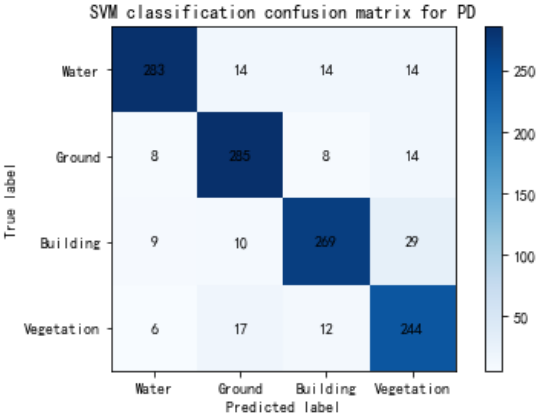

(c)

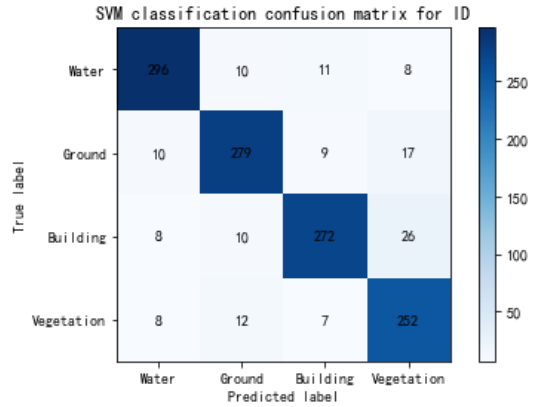

(d)

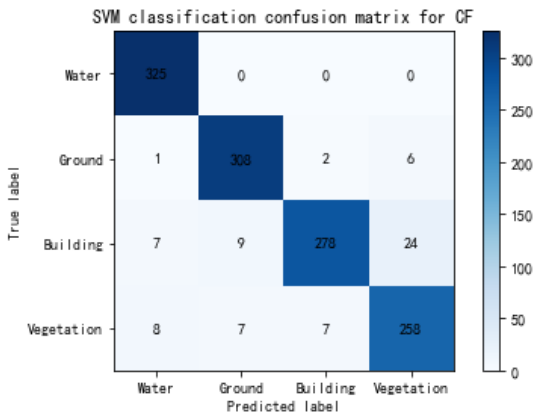

(e)

Figure 12. Confusion matrix of different methods, Where Fig.12 (a) is the confusion matrix of EI, Fig.12 (b) is the confusion matrix of ET, Fig.12(c) is the confusion matrix of PD, Fig.12 (d) is the confusion matrix of ID, Fig.12 (e) is the confusion matrix of Feature combination.

Class	EI	ET	PD	ID	CF
Water	88%	89%	87%	91%	100%
Ground	92%	91%	90%	88%	97%
Building	84%	86%	88%	89%	91%
Vegetation	82%	89%	87%	90%	92%
Total Number	87%	88%	88%	89%	95%

Table 3. Accuracy results of identification

The coastline is extracted by ground and water binary images. In the experimental results, the confusion matrix comes from the experimental classifier. In the meanwhile, the accuracy of water and land division is verified, therefore, the coastline can be extracted successfully. In addition, the coastline obtained from deep learning classification is further compared with that obtained by DTM to verify the feasibility as Table 4.

Coastline extraction method	Coastline extraction based on terrain classification	Coastline extraction based on DEM
Coastline movement(meter)	32.86	31.97

Table 4. Comparison of coastline movement extracted by two methods

5.2.3 Uncertain influencing factors: About the uncertain analysis, it will be better if the data were derived in late October 2012 and early November 2012, which is close to the day when Sandy made landfall and departed. We cannot determine all these coastal erosion changes due to Hurricane Sandy, there must be some erosion influenced by other factors. That's to say, time resolution and timeliness should be raised.

6. CONCLUSION

Hurricane Sandy brought severe disaster to Fire Island, which changed the whole island completely. This work disclosed the distribution of coastal erosion and sediment accumulation and coastline movement. At present, GIS and RS have become vital tools in studying abnormal phenomena related to change detection. Compared with ordinary images, LiDAR has the characteristics of higher resolution and stronger anti-interference ability. In conclusion, by using GIS methods to process LiDAR point cloud data, we acquire Elevation Change Model and implement the visualization to clarify the law and scope of sediment and erosion. Through PCA weight determination and SVM classification, the coastline is extracted and the movement distance of coastline is obtained by machine learning of multi-feature extraction. The feasibility of this method is also confirmed by comparing the parameters of various methods. There are various parameters that are significant when processing the point clouds data and deep learning, although a few of parameters are mentioned in the previous discussion. We hope that people can have a better and deeper understanding of the seriousness of coastal erosion and improve the awareness of disaster prevention through this study.

This contribution has been peer-reviewed. The double-blind peer-review was conducted on the basis of the full paper.
https://doi.org/10.5194/isprs-annals-V-3-2022-569-2022 | © Author(s) 2022. CC BY 4.0 License.

ACKNOWLEDGEMENT

Authors would like to thank Dr. Jonathan Resop for his thoughtful guidance and anonymous reviewers for their constructive comments. This study was financially supported by the geological data related programs of China Geological Survey DD20190428, National Key R&D Program of China (2016YFC0600600), China Geological Survey Project (DD20190450, DD20190451), National Nonprofit Institute Research Grant of IGGE (AS2022P03).

REFERENCES

Bishop, C.M. (1999) 'Bayesian pca', *Advances in neural information processing systems*, MIT; 1998, 382–388.

Cui, Y. (2020) 'Lane change identification and prediction with roadside LiDAR data', *Optics and Laser Technology*, 9.

Dolan, R., Hayden, B. & Heywood, J. (1978) 'Analysis of coastal erosion and storm surge hazards', *Coastal Engineering*, 2, 41–53.

Felix, R. (n.d.) 'Point Density and Point Spacing', *Felix Rohrbach*. Available at: http://felix.rohrba.ch/en/2015/point-density-and-point-spacing/.

Gálai, B. & Benedek, C. (2017) 'Change Detection in Urban Streets by a Real Time Lidar Scanner and MLS Reference Data', in Karray, F., Campilho, A., and Cheriet, F. (eds) *Image Analysis and Recognition*, Cham: Springer International Publishing (Lecture Notes in Computer Science), 210–220.

Gibson, L., Adeleke, A., Hadden, R. & Rush, D. (2020) 'Spatial metrics from LiDAR roof mapping for fire spread risk assessment of informal settlements in Cape Town, South Africa', *Fire Safety Journal*, 103053.

Goff, J.A., Flood, R.D., Austin Jr., J.A., Schwab, W.C., Christensen, B.A., Browne, C.M., Denny, J.F. & Baldwin, W.E. (2015) 'The impact of Hurricane Sandy on the shoreface and inner shelf of Fire Island, New York: large bedform migration but limited erosion', *Continental Shelf Research*, 98, 13.

Gracia, A., Rangel-Buitrago, N., Oakley, J.A. & Williams, A.T. (2018) 'Use of ecosystems in coastal erosion management', *Ocean & Coastal Management*, 156, 277–289.

Hsu, S.A. (2013) 'Storm Surges in New York During Hurricane Sandy in 2012: A Verification of the Wind-Stress Tide Relation', *Boundary-Layer Meteorology*, 148, 593–598.

Kerguillec, R., Audère, M., Baltzer, A., Debaine, F., Fattal, P., Juigner, M., Launeau, P., Le Mauff, B., Luquet, F., Maanan, M., Pouzet, P., Robin, M. & Rollo, N. (2019) 'Monitoring and management of coastal hazards: Creation of a regional observatory of coastal erosion and storm surges in the pays de la Loire region (Atlantic coast, France)', *Ocean & Coastal Management*, 181, 104904.

Krishnan, A.K., Nissen, E., Saripalli, S., Arrowsmith, R. & Hinojosa-Corona, A. (n.d.) 'Change Detection Using Airborne LiDAR: Applications to Earthquakes', 11.

Leatherman, S.P., Zhang, K. & Douglas, B.C. (2000) 'Sea level rise shown to drive coastal erosion', *Eos, Transactions American Geophysical Union*, 81, 55.

Lee, J., Cai, X., Lellmann, J., Dalponte, M., Malhi, Y., Butt, N., Morecroft, M., Schönlieb, C.-B. & Coomes, D.A. (2016) 'Individual tree species classification from airborne multisensor imagery using robust PCA', *IEEE Journal of Selected Topics in Applied Earth Observations and Remote Sensing*, IEEE, 9, 2554–2567.

Lentz, E.E., Hapke, C.J., Stockdon, H.F. & Hehre, R.E. (2013) 'Improving understanding of near-term barrier island evolution through multi-decadal assessment of morphologic change', *Marine Geology*, 337, 125–139.

Li, H., Gu, H., Han, Y. & Yang, J. (2007) 'Fusion of high-resolution aerial imagery and lidar data for object-oriented urban land-cover classification based on svm', in *ISPRS Workshop on Updating Geo-spatial Databases with Imagery & The 5th ISPRS Workshop on DMGISs*, Citeseer.

Li, R., Liu, J.-K. & Felus, Y. (n.d.) 'Spatial Modeling and Analysis for Shoreline Change Detection and Coastal Erosion Monitoring', 13.

Lodha, S.K., Kreps, E.J., Helmbold, D.P. & Fitzpatrick, D. (2006) 'Aerial LiDAR data classification using support vector machines (SVM)', in *Third International Symposium on 3D Data Processing, Visualization, and Transmission (3DPVT'06)*, IEEE, 567–574.

Maglione, P., Parente, C. & Vallario, A. (2014) 'Coastline extraction using high resolution WorldView-2 satellite imagery', *European Journal of Remote Sensing*, 47, 685–699.

Marfai, M.A. (2011) 'The hazards of coastal erosion in Central Java, Indonesia: An overview', 9.

Matkan, A.A., Hajeb, M. & Sadeghian, S. (2014) 'Road extraction from lidar data using support vector machine classification', *Photogrammetric Engineering & Remote Sensing*, American Society for Photogrammetry and Remote Sensing, 80, 409–422.

Mohd, F.A., Abdul Maulud, K.N., Begum, R.A., Selamat, S.N. & A. Karim, O. (2018) 'Impact of Shoreline Changes to Pahang Coastal Area by using Geospatial Technology', *Sains Malaysiana*, 47, 991–997.

Obu, J., Lantuit, H., Grosse, G., Günther, F., Sachs, T., Helm, V. & Fritz, M. (2017) 'Coastal erosion and mass wasting along the

Canadian Beaufort Sea based on annual airborne LiDAR elevation data', *Geomorphology*, 293, 331–346.

Pan, S., Guan, H., Yu, Y., Li, J. & Peng, D. (2019) 'A comparative land-cover classification feature study of learning algorithms: DBM, PCA, and RF using multispectral LiDAR data', *IEEE Journal of Selected Topics in Applied Earth Observations and Remote Sensing*, IEEE, 12, 1314–1326.

Petersburg, St. (2015) *Graphics and photos showing overwash characteristics of 3 locations*.

Prasad, D.H. & Kumar, N.D. (2014) 'Coastal Erosion Studies—A Review', *International Journal of Geosciences*, 05, 341–345.

Samadzadegan, F., Bigdeli, B. & Ramzi, P. (2010) 'A multiple classifier system for classification of LIDAR remote sensing data using multi-class SVM', in *International Workshop on Multiple Classifier Systems*, Springer, 254–263.

Sebek, K., Jacobson, L., Wang, J., Newton-Dame, R. & Singer, J. (2014) 'Assessing Capacity and Disease Burden in a Virtual Network of New York City Primary Care Providers Following Hurricane Sandy', *Journal of Urban Health*, 91, 615–622.

Shi, X. & Zakhor, A. (2011) 'Fast approximation for geometric classification of LiDAR returns', in *2011 18th IEEE International Conference on Image Processing*, IEEE, 2925–2928.

Silke, K. (2012) *LAStools*, Friedrichshafener Straße 1, GERMANY.

Sofonia, J., Phinn, S., Roelfsema, C. & Kendoul, F. (2019) 'Observing Geomorphological Change on an Evolving Coastal Sand Dune Using SLAM-Based UAV LiDAR', *Remote Sensing in Earth Systems Sciences*, 2, 273–291.

Swift, D.J. (1968) 'Coastal erosion and transgressive stratigraphy', *The Journal of Geology*, 76, 444–456.

Swift, D.J.P. & Thorne, J.A. (1991) 'Sedimentation on continental margins, I: a general model for shelf sedimentation', *Shelf Sand and Sandstone Bodies, Geometry, Facies and Sequence Stratigraphy*, 14, 3–31.

Vapnik, V. (1999) *The nature of statistical learning theory*, Springer science & business media.

Vapnik, V.N. (1999) 'An overview of statistical learning theory', *IEEE transactions on neural networks*, IEEE, 10, 988–999.

Varlas, G., Papadopoulos, A. & Katsafados, P. (2019) 'An analysis of the synoptic and dynamical characteristics of hurricane Sandy (2012)', *Meteorology and Atmospheric Physics*, 131, 443–453.

Xian, J., Sun, D., Xu, W., Han, Y., Zheng, J., Peng, J. & Yang, S. (2020) 'Urban air pollution monitoring using scanning Lidar', *Environmental Pollution*, 258, 113696.

Zhu, X., Wang, C., Nie, S., Pan, F., Xi, X. & Hu, Z. (2020) 'Mapping forest height using photon-counting LiDAR data and Landsat 8 OLI data: A case study in Virginia and North Carolina, USA', *Ecological Indicators*, 114, 106287.